TSINGHUA SCIENCE AND TECHNOLOGY
ISSN 1007-0214 17/22 pp207–215
DOI: 10.26599/TST.2022.9010070
Volume 29, Number 1, February 2024

980 nm Near-Infrared Light-Emitting Diode Using All-Inorganic Perovskite Nanocrystals Doped with Ytterbium Ions

Zhenglan Ye†, Taoran Liu†, Dan Chen, Yazhou Yang, Jiayi Li, Yaqing Pang, Xiangquan Liu, Yuhua Zuo*, Jun Zheng, Zhi Liu, and Buwen Cheng

Abstract: All-inorganic perovskite ($CsPbX_3$) nanocrystals (NCs) have recently been widely investigated as versatile solution-processable light-emitting materials. Due to its wide-bandgap nature, the all-inorganic perovskite NC Light-Emitting Diode (LED) is limited to the visible region (400–700 nm). A particularly difficult challenge lies in the practical application of perovskite NCs in the infrared-spectrum region. In this work, a 980 nm NIR all-inorganic perovskite NC LED is demonstrated, which is based on an efficient energy transfer from wide-bandgap materials ($CsPbCl_3$ NCs) to ytterbium ions (Yb^{3+}) as an NIR emitter doped in perovskite NCs. The optimized $CsPbCl_3$ NC with 15 mol%Yb^{3+} doping concentration has the strongest 980 nm photoluminescence (PL) peak, with a PL quantum yield of 63%. An inverted perovskite NC LED is fabricated with the structure of ITO/PEDOT: PSS/poly-TPD/$CsPbCl_3$:15 mol%Yb^{3+} NCs/TPBi/LiF/Al. The LED has an External Quantum Efficiency (EQE) of 0.2%, a Full Width at Half Maximum (FWHM) of 47 nm, and a maximum luminescence of 182 cd/m^2. The introduction of Yb^{3+} doping in perovskite NCs makes it possible to expand its working wavelength to near-infrared band for next-generation light sources and shows potential applications for optoelectronic integration.

Key words: perovskite nanocrystals; rare-earth doping; Light-Emitting Diode (LED); near-infrared; optical interconnection

1 Introduction

All-inorganic perovskite ($CsPbX_3$) nanocrystals (NCs) have recently been widely investigated as versatile solution-processable photonic sources for displays, lighting, Light-Emitting Diodes (LEDs), lasers[1–7], and photodetectors[8, 9]. Perovskite NCs have many special advantages, such as high PhotoLuminescence Quantum Yield (PLQY) and tunable and narrow emission bandwidth with convenient, low-cost, and solution-based integration on any substrate[10–13] due to their quantum-size effects, surface engineering, and

• Zhenglan Ye, Dan Chen, Yazhou Yang, Jiayi Li, Yaqing Pang, Xiangquan Liu, Yuhua Zuo, Jun Zheng, Zhi Liu, and Buwen Cheng are with the State Key Laboratory on Integrated Optoelectronics, Institute of Semiconductors, Chinese Academy of Sciences, Beijing 100083, China, and also with the Center of Materials Science and Optoelectronics Engineering, University of Chinese Academy of Sciences, Beijing 100049, China. E-mail: yezhenglan@semi.ac.cn; chendan1988@semi.ac.cn; yangyazhou@semi.ac.cn; lijiayi@semi.ac.cn; pyq@semi.ac.cn; liuxiangquan@semi.ac.cn; yhzuo@semi.ac.cn; zhengjun@semi.ac.cn; zhiliu@semi.ac.cn; cbw@semi.ac.cn.
• Taoran Liu is with the State Key Laboratory on Integrated Optoelectronics, Institute of Semiconductors, Chinese Academy of Sciences, Beijing 100083, China, and with the Center of Materials Science and Optoelectronics Engineering, University of Chinese Academy of Sciences, Beijing 100049, China, and also with the Intelligent Network Research Institute, Zhejiang Lab, Hangzhou 311100, China. E-mail: trliu@zhejianglab.com.
† Zhenglan Ye and Taoran Liu contribute equally to this paper.
* To whom correspondence should be addressed.
Manuscript received: 2022-10-20; revised: 2022-12-26; accepted: 2022-12-29

shape engineering[14]. NC, also called Quantum Dot (QD) Light-Emitting Devices (namely QLEDs) have been favored by many visionary companies owing to their high color purity, and cost-effectiveness compared with traditional Organic Light-Emitting Device (OLED) counterparts[7]. Moreover, according to the North American National Television Standards Committee, the color gamut of QLEDs reaches up to 140%, which transcends that of typical OLED displays[15]. However, due to the fundamental bandgap restrictions, most perovskite LEDs are limited to the visible region (400–700 nm)[16, 17]. A particularly difficult challenge lies in the practical application of perovskite NCs in the infrared-spectrum region. Near-infrared (namely NIR) LEDs have wide applications in optical communications[18], optical interconnections[18], night-vision devices[19], and biological imaging[20]. How to extend the working wavelength of perovskite NC LED from the visible region to NIR is a key problem. When using FA ion to replace Cs ion, $FAPbI_3$ NC LED exhibits an emitting peak at 772 nm, but with an External Quantum Efficiency (EQE) of 0.12% for $FA_{0.1}Cs_{0.9}PbI_3$ NCs and EQE of 2.3% for $FAPbI_3$ NCs[21]. One approach is to use multinary compositions (mixed cation and mixed anion), based on the work by Lignos et al.[22] Using $Cs_xFA_{1-x}Pb(Br_{1-y}I_y)_3$ NCs, the LED realizes, an EQE of 5.9% with a bandwidth of 27 nm at 735 nm. However, most works can only extend the wavelength of the first NIR window to 700–900 nm. Owing to the limits of perovskite cations and anions, longer than 900 nm perovskite NC LEDs can be hardly realized. In this paper, a 980 nm NIR all-inorganic perovskite NC LED is first demonstrated, which is based on an efficient energy transfer from wide-bandgap materials ($CsPbCl_3$ NCs) to ytterbium ions (Yb^{3+}) as an NIR emitter doped in perovskite NCs.

2 Experiment

2.1 Materials

Indium Tin Oxide (ITO) glasses with a thickness of 1.1 mm and size of $1.5\times1.5\,cm^2$ (square resistance <5 W/sp, transmittance $>85\%$) were purchased from South China Science & Technology Company Limited. Octadecene (ODE, 90.000%), oleylamine (OAm, 80 – 90%), n-hexane (97.000%), and ethyl acetate (99.8%) were all purchased from Sigma-Aldrich. Oleic acid (OA, 90.000%) was purchased from Alfa Aesar. CsOAc (99.99%), $Pb(QAc)_2{\cdot}3H_2O$ (99.998%), $Yb(QAc)_3{\cdot}4H_2O$ (99.9%), and chlorotrimethylsilane (TMSC, 99.0%) were all purchased from Aladdin. Acetone (99.500%), ethanol (99.700%), isopropanol (99.700%), and toluene (99.5%) were all purchased from Beijing Chemical Works. Chlorobenzene (99.5%) was purchased from Shanghai MaterWin New Materials Co., Ltd. PEDOT:PSS, poly-TPD, TPBi (>99%), and LiF (>99.0%) were purchased from Xi'an Polymer Optical Technology Corp (Xi'an, China). Aluminum (Al, 99.99%) was purchased from China New Metal Materials Technology Co., Ltd.

2.2 Perovskite NC preparation

2.2.1 Preparation of precursors

CsOAc precursor: 4 mmol (0.76 g) of CsOAc powder was dissolved in 4 mL anhydrous ethanol and stirred at 60 °C for 20 mins until the powder was fully dissolved to prepare the 1 mol/L CsOAc ethanol precursor solution.

TMCS precursor: 2 mL of TMSC and 5 mL of ODE were mixed together to prepare the TMCS precursor solution.

2.2.2 Preparation of perovskite NCs

Preparation of the crude nanocrystalline solution: $CsPbCl_3$ NCs with a Yb/Pb ratio of 1.5 mmol/2 mmol were taken as an example, which was used to synthesize the 15 mol% doped $CsPbCl_3$:Yb^{3+} NCs. 2 mmol of $Pb(OAC)_2{\cdot}3H_2O$ and 1.5 mmol of $Yb(OAC)_3{\cdot}4H_2O$ and 10 mL of OA and 6 mL of OAM and 50 mL of ODE and 2.8 mL of the CsOAc ethanol precursor solution were mixed together in a 250 mL quartz three-neck flask, and the mixture was degassed with a vacuum pump for 5 mins at room temperature. Then, dry nitrogen (N_2) was charged into the flask, and the solution was heated to 110 °C. The degassing step was repeated again for 1–2 h until the powder was completely dissolved in the mixed solution. Afterward, the temperature of the solution was raised to 180–240 °C in the N_2 environment. The TMCS precursor solution was rapidly injected into the flask. Then, the flask was immediately placed in an ice-water bath after 5 s of reaction to obtain a crude solution of $CsPbCl_3$:Yb^{3+} NCs.

Cleaning and purification of NCs: After centrifuging the crude NC solution at 12 000 rpm for 10 mins, the supernatant was discarded. The precipitate was ultrasonically dispersed in a mixed solution of ethyl acetate and n-hexane (1:1) and centrifuged at 12 000 rpm for 10 mins. The ultrasonic dispersion and centrifugation steps were repeated again. Then the supernatant was discarded, and the precipitate

was dispersed in n-hexane to obtain the $CsPbCl_3$:Yb^{3+} NC solution.

2.3 Device fabrication

A 1.5 cm × 1.5 cm ITO/glass substrate was ultrasonically cleaned in acetone, isopropanol and ethanol solutions, then washed with deionized water and dried with N_2. Subsequently, the substrate was placed under an ultraviolet-ozone environment for 20 mins. The PEDOT:PSS solution and the poly-TPD chlorobenzene solution (8 mg/mL) were stirred at room temperature for more than 2 h and then filtrated with a 0.45 μm filter. 80 μL of the PEDOT:PSS solution was spin-coated on the ITO at 4000 rpm for 60 s, followed by annealing at 140 °C for 15 mins. In the glove box, 100 μL of the poly-TPD solution was spin-coated on the PEDOT:PSS layer at 1000 rpm for 60 s, followed by annealing at 150 °C for 20 mins. 100 μL of the $CsPbCl_3$:Yb^{3+} NC solution was spin-coated on the poly-TPD layer at 5000 rpm for 60 s. TPBi with a thickness of 50 nm and LiF with a thickness of 1–2 nm and patterned Al electrodes with a thickness of 80–100 nm were successively evaporated onto the substrate using a thermal evaporation system integrated into the glove box. The $CsPbCl_3$: 15 mol%Yb^{3+} NC LED device was successfully fabricated with effective emission areas of 4 mm^2. All devices were measured under ambient conditions without encapsulation.

2.4 Characterization

The morphologies of perovskite NCs were observed using a Transmission Electron Microscope (TEM) (Talos F200X) made by FEI Corp., and the device cross section was obtained through Scanning Elecgtron Microscopy (SEM) using a high-resolution scanning ZEISS microscope. X-Ray Diffraction (XRD) analysis was studied by Bruker D8 Focus (Bruker Corporation, Germany) to determine the crystal structures of the perovskite NCs. The effective Yb^{3+} content was obtained using an Inductively Coupled Plasma Optical Emission Spectrometer (ICP-OES) (PerkinElmer Optima 8300). The optical absorption properties of the NC samples were obtained using a Shimadzu UV-3600i Plus UV-vis-NIR spectrophotometer (330–1100 nm). The PL spectra and Time-Resolved PhotoLuminescence (TRPL) decay spectra of the NCs were investigated using the FLS920 fluorescence spectrometer (Edinburgh Instruments (EI)). The current-voltage properties were studied using Keysight 2902A. The EL spectrum and EQE of the LED were determined using integrated measuring equipment from Ocean Insight.

3 Result and Discussion

$CsPbCl_3$ NC samples with different Yb^{3+}-doped conditions were prepared, and the effective Yb^{3+}-doped concentrations are shown in Table 1. First, when the initial molar weight of Yb^{3+} was less than 1.5 mmol, the effective Yb^{3+} doping concentration increased from 4.5 mol% to 15.37 mol%, with the increase of the initial molar weight of Yb^{3+}. However, when it was as high as 2 mmol (doped concentration of 100%), the effective Yb^{3+} doping concentration sharply decreased to only 5.5 mol%. Hence, at a too-high doping content, most Yb^{3+} ions may locate at interstitial sites instead of substitution sites. The optimized effective Yb^{3+} doping concentration in $CsPbCl_3$ NCs is approximately 15 mol%.

As shown in Fig. 1a, with Yb^{3+} doped in $CsPbCl_3$ NCs, the PL peak intensity of 410 nm obviously decreased. Hence, the energy transfers from $CsPbCl_3$ NCs to Yb^{3+}. The strongest quenching happened to the NC sample with 15 mol% Yb^{3+}. The emission peak intensity was lower for the sample with 4.5 mol% Yb^{3+} compared to that with 5.5 mol% Yb^{3+}. It may be caused by the weakened energy transfer due to the excessive Yb^{3+} ions in interstitial sites. The $CsPbCl_3$:15 mol%Yb^{3+} has the best energy transfer efficiency, which can also be proved in Fig. 1b, with the strongest PL peak intensity of 980 nm. Thus, $CsPbCl_3$:15 mol%Yb^{3+} NCs were chosen as the active layer for LEDs in the following text.

Figure 2 shows the TEM and High-Resolution Transmission Electron Microscopy (HRTEM) test results of the undoped and $CsPbCl_3$:15 mol%Yb^{3+} NCs. As shown in Figs. 2e and 2f, the average particle size of the doped and undoped NCs is 13.88 nm and 14.69 nm, respectively. The corresponding lattice spacing is 5.48 Å and 5.62 Å, respectively, as shown in Figs. 2b and 2c. The particle size and lattice spacing of the doped samples were slightly smaller because of the slight compression of perovskite lattice resulting from the substitution of Yb^{3+} ions with a smaller ion radius (87 pm) as compared

Table 1 Elemental concentrations of Yb^{3+}-doped perovskite nanocrystals measured via ICP-OES.

Condition (240 °C, Pb^{2+} 2 mmol)	mol(%) (Yb/Pb) (Effective Yb^{3+} doping concentration)
Yb^{3+} – 1 mmol (50% Pb^{2+})	4.50
Yb^{3+} – 1.5 mmol (75% Pb^{2+})	15.37
Yb^{3+} – 2 mmol (100% Pb^{2+})	5.50

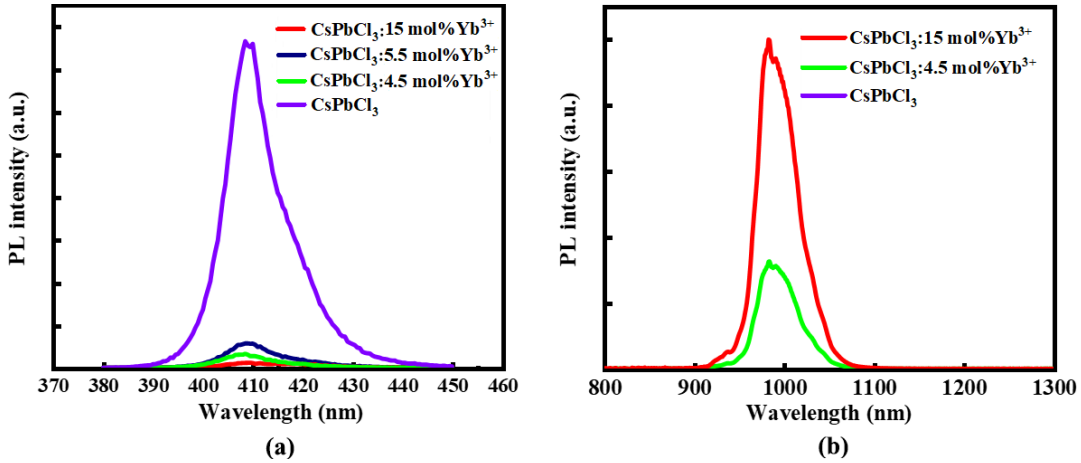

Fig. 1 PL test results of $CsPbCl_3$ NCs with different Yb^{3+} contents (a) in the visible and (b) NIR regions.

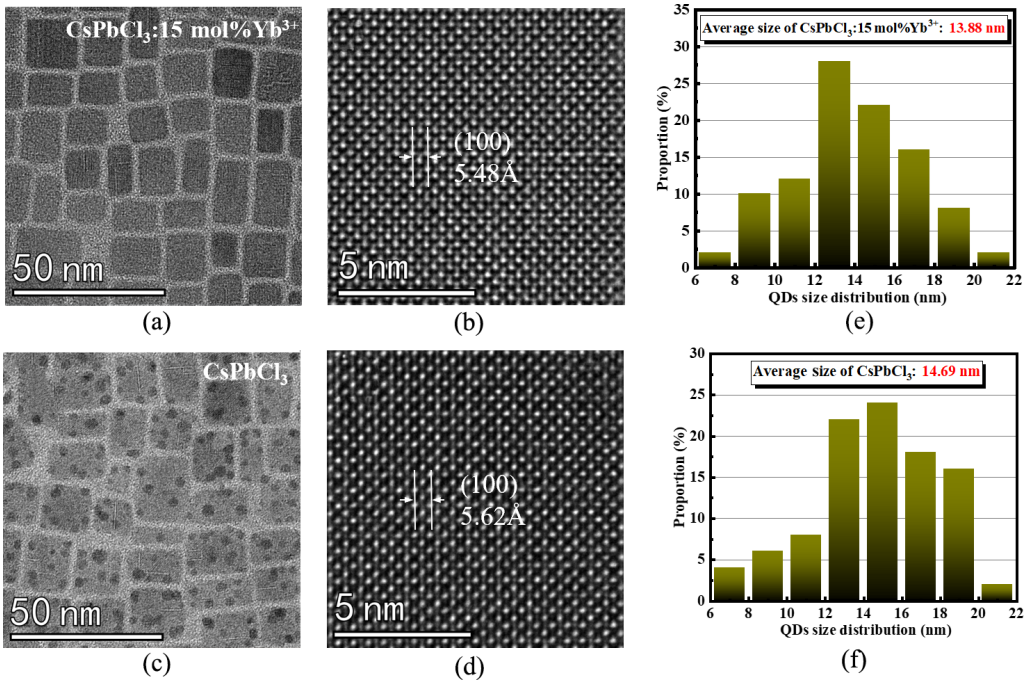

Fig. 2 TEM test results of the Yb^{3+}-doped and undoped NCs, (a) and (c) are TEM images, (b) and (d) are HRTEM images, and (e) and (f) are particle size statistics.

to Pb^{2+} ions (119 pm). This condition can also be confirmed by the slight blue shift of the visible-light emission peak in the PL curves in Fig. 3a.

The XRD results of the perovskite NC films are shown in Fig. 3c. The diffraction peaks of $CsPbCl_3$:15 mol%Yb^{3+} NC sample still roughly match the PDF card of undoped $CsPbCl_3$ NCs of the cubic phase. However, the slight shifts (0.26° and 0.40°) of the diffraction peaks corresponding to the (110) and (200) crystal planes in the XRD image indicate that the doping of Yb^{3+} leads to a slight change in the internal lattice structure of the $CsPbCl_3$ NCs.

The PL test results of the undoped and $CsPbCl_3$:15 mol%Yb^{3+} NCs films in the visible and NIR bands are shown in Fig. 3a. The thin films exhibit double PL peaks at 407 nm and 980 nm, which correspond to the luminescence of $CsPbCl_3$ NCs and Yb^{3+} energy levels respectively. Compared with the undoped sample, the $CsPbCl_3$:15 mol%Yb^{3+} NC film exhibits luminescence quenching of the intrinsic $CsPbCl_3$ peak (~410 nm) due to the energy transfer to the Yb^{3+} energy level. The excitons were excited to the $CsPbCl_3$ excited state with the absorption of 365 nm photons. Then, the subsequent radiative recombination process generates

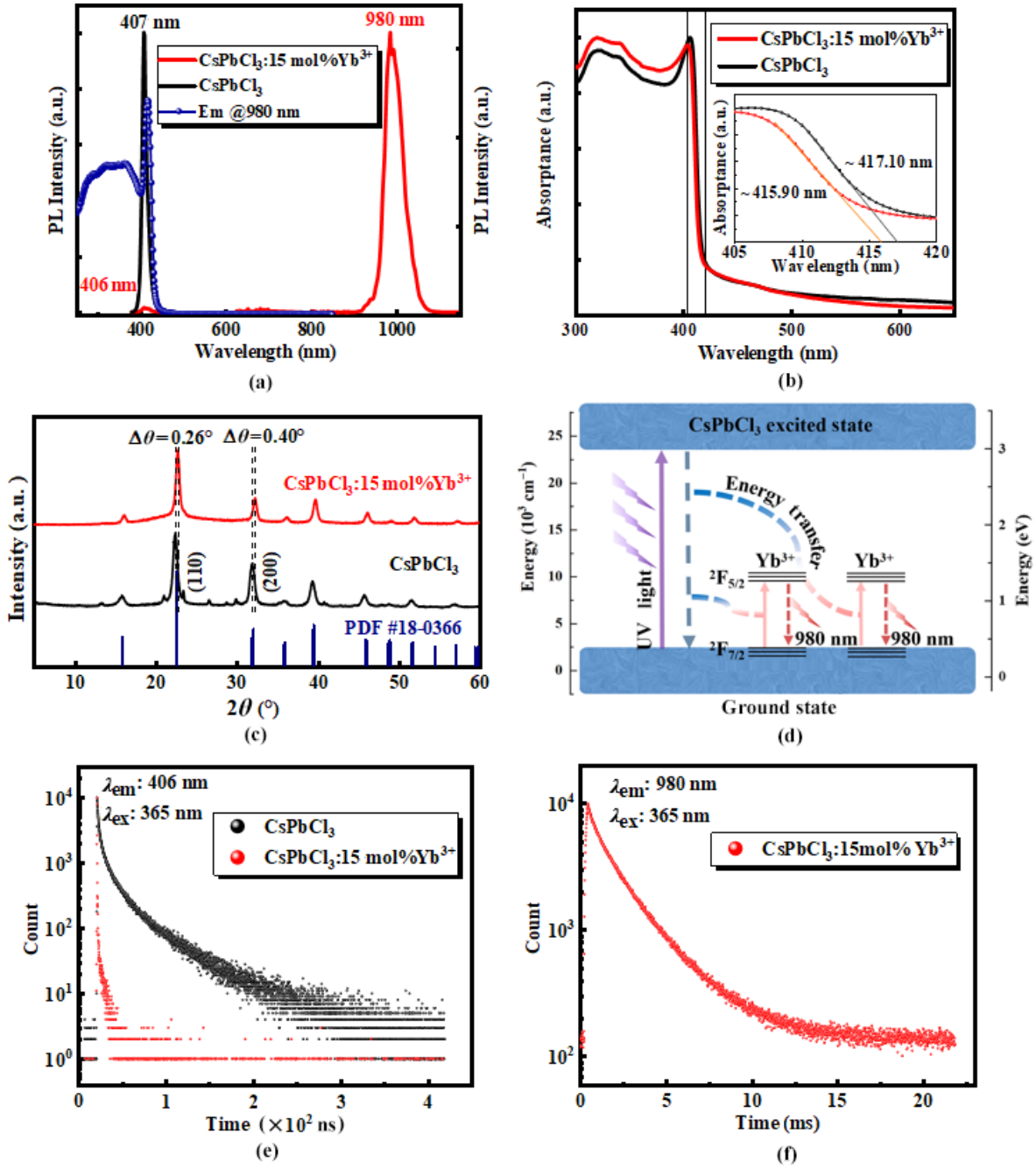

Fig. 3 Optical characterizations of the perovskite nanocrystals. (a) PL and excitation spectra, (b) absorption spectra, (c) XRD results, (d) schematic diagram of the inner energy transfer progress, (e) visible-band TRPL spectra of the undoped and $CsPbCl_3$:15 mol%Yb^{3+} NC films, and (f) TRPL spectra of $CsPbCl_3$:15 mol%Yb^{3+} NC films at 980 nm.

410 nm photons, whose energy will be transferred to Yb^{3+} ions, and 980 nm double photons will be released. Through this quantum cutting effect, the PLQY can reach 200% theoretically. The absorption spectra of the undoped and $CsPbCl_3$:15 mol%Yb^{3+} NC films are shown in Fig. 3b, which exhibit strong absorption in the entire UV band. The PLQY of 980 nm was over 60% excited by 310 nm, which lays a foundation for electroluminescence at the NIR band.

The TRPL spectra results are shown in Figs. 3e and 3f. The average lifetime was calculated through exponential decay fitting from the TRPL spectra. The visible-band lifetimes of the undoped and $CsPbCl_3$:15 mol%Yb^{3+} NCs are 4.29 ns and 0.39 ns, respectively, caused by the rare-earth energy level as a radiative recombination center. Meanwhile, the 1.80 ms lifetime of $CsPbCl_3$:15

mol%Yb^{3+} NCs at 980 nm shown in Fig. 3f is one of the typical features of the Yb^{3+} "$^2F_{5/2}$ to $^2F_{7/2}$" radiative recombination, as shown in Fig. 3d.

Here, the NIR LED using $CsPbCl_3$:15 mol%Yb^{3+} NCs as the light-emitting layer was successfully fabricated. The device with an inverted structure is shown in Fig. 4a, consisting of ITO/PEDOT:PSS/poly-TPD/$CsPbCl_3$:15 mol%Yb^{3+} NCs/TPBi (50 nm)/LiF(1 nm)/Al(100 nm). The energy band diagram of the LED is shown in Fig. 4b. The cross-sectional SEM image of the LED is shown in Fig. 4c, which indicates a successful deposition of all layers. From the photo of the LED in Fig. 4d, it can be measured that the effective light-emitting area of the LED is 4 mm^2.

The electrical characteristics of the $CsPbCl_3$:15 mol%Yb^{3+} NC LED are shown in Fig. 5. 980 nm electroluminescence variations with excitation bias voltages are shown in Fig. 5a. As shown in Figs. 5b to 5d, the turn-on voltage is 6.5 V, and the maximum EQE is 0.2% at an external voltage of 7.5 V with a luminescent brightness of 162 cd/m^2. Meanwhile, the maximum luminescent brightness of 182 cd/m^2 was achieved at a voltage of 8.5 V. A relatively low luminescent brightness may result from the reduced carrier transport in the electron/hole transport layers[22], which can be mitigated by engineering the surface of the NCs in future works. The charge-transport problem was also reflected at the high turn-on voltage ($\geqslant$ 6.5 V). As shown in Figs. 5b and 5d, the EL intensity decays with the increase in the bias voltage after 8.5 V, while the current still increases. Similar phenomena have been observed for green LED devices[16, 17]. Due to the sensitivity to the temperature and electrical stress of perovskite NCs, deterioration occurs in the perovskite layer with increasing voltage, with the heating loss caused by the larger current.

The 0.2% EQE of the 980 nm perovskite NC LED is actually lower than 5.9%[23] of the 980 nm perovskite LED with Yb^{3+}-doped $CsPbCl_3$ films. The main reason is due to the poor electrical injection for NCs, caused by the insulation nature of long-chain organic ligands on the surface of NCs. One method to improve the performance is to clean the surface of NCs using a weak polar solvent, such as ethyl acetate, but its effect is not satisfied[24–26]. In addition, $CsPbCl_3$ NCs are quite sensitive to defects, and the surface defects between the NC layer and electron or hole transfer layer can cause severe luminescence quenching[27–30].

4 Conclusion

The LED based on $CsPbCl_3$:15 mol%Yb^{3+} NCs realizes an NIR electroluminescence of 980 nm, with an EQE of 0.2%, a full width at half maximum of 47 nm, and a maximum luminescence of 182 cd/m^2. The introduction of Yb^{3+} doping in perovskite NCs expands its working wavelength in the NIR for next-generation light-emitting sources.

Acknowledgment

This work was supported by the National Key Research and Development Program of China (No. 2018YFB2200103)

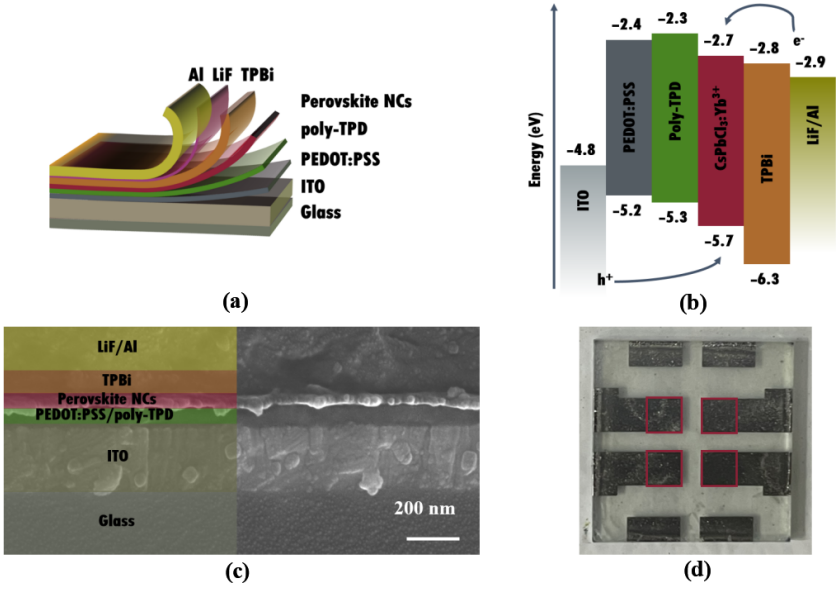

Fig. 4 Structural diagrams of the PeLED device. (a) 3D layer diagram, (b) schematic diagram of the energy band structure, (c) cross-sectional SEM image, and (d) photo of the $CsPbCl_3$:15 mol%Yb^{3+} NC LED.

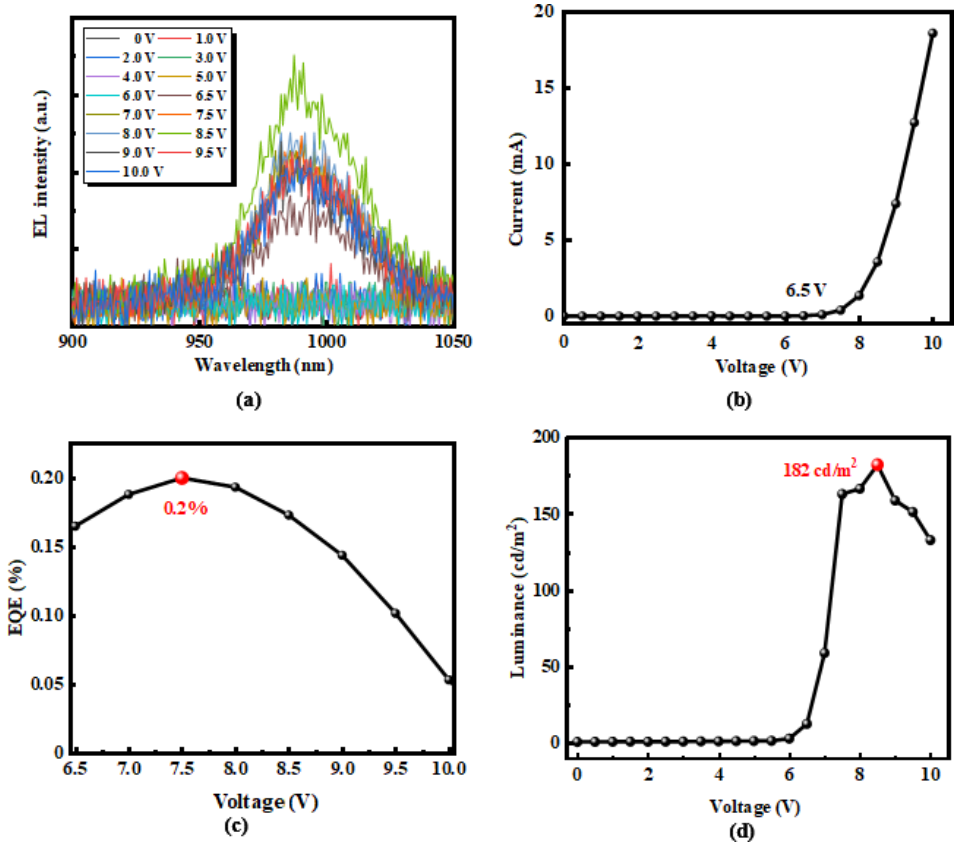

Fig. 5 Electrical characterizations of the PeLED device. (a) EL intensity-wavelength under different voltages, (b) current-voltage, (c) EQE-voltage, and (d) luminescence-voltage characteristics of a $CsPbCl_3:Yb^{3+}$ (15 mol%) based LED.

and the National Natural Science Foundation of China (Nos. 61875186 and 62250010).

References

[1] X. K. Liu, W. Xu, S. Bai, Y. Jin, J. Wang, R. H. Friend, and F. Gao, Metal halide perovskites for light-emitting diodes, *Nat. Mater.*, vol. 20, no. 1, pp. 10–21, 2021.

[2] H. Tsai, S. Shrestha, R. A. Vilá, W. Huang, C. Liu, C. H. Hou, H. H. Huang, X. Wen, M. Li, G. Wiederrecht, et al., Bright and stable light-emitting diodes made with perovskite nanocrystals stabilized in metal-organic frameworks, *Nat. Photonics*, vol. 15, no. 11, pp. 843–849, 2021.

[3] X. Zhao, J. De Andrew Ng, R. H. Friend, and Z. K. Tan, Opportunities and challenges in perovskite light-emitting devices, *ACS Photonics*, vol. 5, no. 10, pp. 3866–3875, 2018.

[4] X. Li, X. Gao, X. Zhang, X. Shen, M. Lu, J. Wu, Z. Shi, V. L. Colvin, J. Hu, X. Bai, et al., Lead-free halide perovskites for light emission: Recent advances and perspectives, *Adv. Sci.*, vol. 8, no. 4, p. 2003334, 2021.

[5] A. Ren, H. Wang, W. Zhang, J. Wu, Z. Wang, R. V. Penty, and I. H. White, Emerging light-emitting diodes for next-generation data communications, *Nat. Electron.*, vol. 4, no. 8, pp. 559–572, 2021.

[6] H. Jung, N. Ahn, and V. I. Klimov, Prospects and challenges of colloidal quantum dot laser diodes, *Nat. Photonics*, vol. 15, no. 9, pp. 643–655, 2021.

[7] Y. F. Li, J. Feng, and H. B. Sun, Perovskite quantum dots for light-emitting devices, *Nanoscale*, vol. 11, no. 41, pp. 19119–19139, 2019.

[8] L. Zhou, K. Yu, F. Yang, J. Zheng, Y. Zuo, C. Li, B. Cheng, and Q. Wang, All-inorganic perovskite quantum dot/mesoporous TiO_2 composite-based photodetectors with enhanced performance, *Dalton Trans.*, vol. 46, no. 6, pp. 1766–1769, 2017.

[9] X. Liu, T. Liu, D. Chen, Y. Yang, Z. Ye, Y. Zuo, J. Zheng, Z. Liu, and B. Cheng, Broad-spectrum germanium photodetector based on the ytterbium-doped perovskite nanocrystal downshifting effect, *ACS Appl. Opt. Mater.*, vol. 1, no. 1, pp. 507–512, 2023.

[10] Kenry, Y. Duan, and B. Liu, Recent advances of optical imaging in the second near-infrared window, *Adv. Mater.*, vol. 30, no. 47, p. 1802394, 2018.

[11] N. Tessler, V. Medvedev, M. Kazes, S. Kan, and U. Banin, Efficient near-infrared polymer nanocrystal light-emitting diodes, *Science*, vol. 295, no. 5559, pp. 1506–1508, 2002.

[12] K. N. Bourdakos, D. M. N. M. Dissanayake, T. Lutz, S. R. P. Silva, and R. J. Curry, Highly efficient near-infrared hybrid organic-inorganic nanocrystal electroluminescence device, *Appl. Phys. Lett.*, vol. 92, no. 15, p. 153311, 2008.

[13] G. J. Supran, K. W. Song, G. W. Hwang, R. E. Correa, J. Scherer, E. A. Dauler, Y. Shirasaki, M. G. Bawendi, and V. Bulovic, High-performance shortwave-infrared light-emitting devices using core-shell (PbS-CdS) colloidal

quantum dots, *Adv. Mater.*, vol. 27, no. 8, pp. 1437–1442, 2015.
[14] M. V. Kovalenko, L. Manna, A. Cabot, Z. Hens, D. V. Talapin, C. R. Kagan, V. I. Klimov, A. L. Rogach, P. Reiss, D. J. Milliron, et al., Prospects of nanoscience with nanocrystals, *ACS Nano*, vol. 9, no. 2, pp. 1012–1057, 2015.
[15] L. Protesescu, S. Yakunin, M. I. Bodnarchuk, F. Krieg, R. Caputo, C. H. Hendon, R. X. Yang, A. Walsh, and M. V. Kovalenko, Nanocrystals of cesium lead halide perovskites (CsPbX3, X= Cl, Br, and I): Novel optoelectronic materials showing bright emission with wide color gamut, *Nano Lett.*, vol. 15, no. 6, pp. 3692–3696, 2015.
[16] D. Chen, T. Liu, Y. Zuo, C. Li, J. Zheng, Z. Liu, B. Liu, and B. Cheng, Brightness and lifetime improved light-emitting diodes from Sr-doped quasi-two-dimensional perovskite layers, *Tsinghua Science and Technology*, vol. 28, no. 1, pp. 131–140, 2023.
[17] B. Liu, X. Zou, D. Chen, T. Liu, Y. Zuo, J. Zheng, Z. Liu, and B. Cheng, Effect of chloride Ion concentrations on luminescence peak blue shift of light-emitting diode using anti-solvent extraction of quasi-two-dimensional perovskite, *Tsinghua Science and Technology*, vol. 26, no. 4, pp. 496–504, 2021.
[18] G. Konstantatos, I. Howard, A. Fischer, S. Hoogland, J. Clifford, E. Klem, L. Levina, and E. H. Sargent, Ultrasensitive solution-cast quantum dot photodetectors, *Nature*, vol. 442, no. 7099, pp. 180–183, 2006.
[19] L. Sun, J. J. Choi, D. Stachnik, A. C. Bartnik, B. R. Hyun, G. G. Malliaras, T. Hanrath, and F. W. Wise, Bright infrared quantum-dot light-emitting diodes through inter-dot spacing control, *Nat. Nanotechnol.*, vol. 7, no. 6, pp. 369–373, 2012.
[20] I. L. Medintz, H. T. Uyeda, E. R. Goldman, and H. Mattoussi, Quantum dot bioconjugates for imaging, labelling and sensing, *Nat. Mater.*, vol. 4, no. 6, pp. 435–446, 2005.
[21] L. Protesescu, S. Yakunin, S. Kumar, J. Bär, F. Bertolotti, N. Masciocchi, A. Guagliardi, M. Grotevent, I. Shorubalko, M. I. Bodnarchuk, et al., Dismantling the "red wall" of colloidal perovskites: Highly luminescent formamidinium and formamidinium-cesium lead iodide nanocrystals, *ACS Nano*, vol. 11, no. 3, pp. 3119–3134, 2017.
[22] I. Lignos, V. Morad, Y. Shynkarenko, C. Bernasconi, R. M. Maceiczyk, L. Protesescu, F. Bertolotti, S. Kumar, S. T. Ochsenbein, N. Masciocchi, et al., Exploration of near-infrared-emissive colloidal multinary lead halide perovskite nanocrystals using an automated microfluidic platform, *ACS Nano*, vol. 12, no. 6, pp. 5504–5517, 2018.
[23] A. Ishii and T. Miyasaka, Sensitized Yb^{3+} luminescence in CsPbCl3 film for highly efficient near-infrared light-emitting diodes, *Adv. Sci.*, vol. 7, no. 4, p. 1903142, 2020.
[24] H. Wang, N. Sui, X. Bai, Y. Zhang, Q. Rice, F. J. Seo, Q. Zhang, V. L. Colvin, and W. W. Yu, Emission recovery and stability enhancement of inorganic perovskite quantum dots, *J. Phys. Chem. Lett.*, vol. 9, no. 15, pp. 4166–4173, 2018.
[25] C. Zou, C. Y. Huang, E. M. Sanehira, J. M. Luther, and L. Y. Lin, Highly stable cesium lead iodide perovskite quantum dot light-emitting diodes, *Nanotechnology*, vol. 28, no. 45, p. 455201, 2017.
[26] A. Pan, J. Wang, M. J. Jurow, M. Jia, Y. Liu, Y. Wu, Y. Zhang, L. He, and Y. Liu, General strategy for the preparation of stable luminous nanocomposite inks using chemically addressable CsPbX3 peroskite nanocrystals, *Chem. Mater.*, vol. 30, no. 8, pp. 2771–2780, 2018.
[27] T. Fang, T. Wang, X. Li, Y. Dong, S. Bai, and J. Song, Perovskite QLED with an external quantum efficiency of over 21% by modulating electronic transport, *Sci. Bull.*, vol. 66, no. 1, pp. 36–43, 2021.
[28] T. Chiba, Y. Hayashi, H. Ebe, K. Hoshi, J. Sato, S. Sato, Y. J. Pu, S. Ohisa, and J. Kido, Anion-exchange red perovskite quantum dots with ammonium iodine salts for highly efficient light-emitting devices, *Nat. Photonics*, vol. 12, no. 11, pp. 681–687, 2018.
[29] K. Zhang, N. Zhu, M. Zhang, L. Wang, and J. Xing, Opportunities and challenges in perovskite LED commercialization, *J. Mater. Chem. C*, vol. 9, no. 11, pp. 3795–3799, 2021.
[30] J. Huang, M. Lai, J. Lin, and P. Yang, Rich chemistry in inorganic halide perovskite nanostructures, *Adv. Mater.*, vol. 30, no. 48, p. 1802856, 2018.

Dan Chen received the BEng degree from Nanchang University, China in 2011, the MEng degree from Beijing Information Science and Technology University, China in 2018, and the PhD degree from the Institute of Semiconductors, Chinese Academy of Sciences, China in 2021. She is currently a postdoctoral researcher at the Institute of Semiconductors, Chinese Academy of Sciences, China. Her main research interests include perovskite materials and devices, such as solar cells, LEDs, and PDs.

Taoran Liu received the BEng degree from the University of Electronic Science and Technology of China in 2016, and the PhD degree from the Institute of Semiconductors, Chinese Academy of Sciences, China in 2022. She currently works at the Intelligent Network Research Institute of Zhejiang Lab. Her main research interests include perovskite light-emitting materials and devices, the reliability of avalanche photodiodes, and silicon-based NIR photodetectors.

Zhenglan Ye received the BEng degree from Harbin Institute of Technology, China in 2021. He is currently a master student at the Institute of Semiconductors, Chinese Academy of Sciences, China. His main research interests include perovskite LEDs and perovskite X-ray detectors.

Yazhou Yang received the BEng degree from Xiangtan University, China in 2020. He is currently a PhD candidate at the Institute of Semiconductors, Chinese Academy of Sciences, China. His main research interest is perovskite single crystals X-ray detectors.

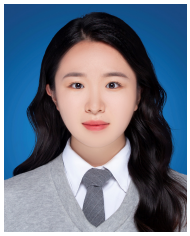

Jiayi Li received the BEng degree from the University of Science and Technology Beijing, China in 2022. She is currently a master student at the Institute of Semiconductors, Chinese Academy of Sciences, China. Her main research interests include perovskite materials and devices.

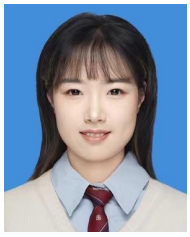

Yaqing Pang received the BEng degree from Hebei University of Technology, China in 2018. She is currently a PhD candidate at the Institute of Semiconductors, Chinese Academy of Sciences, China. Her main research interest is silicon-based avalanche photodetectors.

Xiangquan Liu received the BEng degree from Shandong University of Science and Technology, China in 2017, and the PhD degree from the Institute of Semiconductors, Chinese Academy of Sciences, China in 2022. He is currently a postdoctoral researcher at the Institute of Semiconductors, Chinese Academy of Sciences, China. His main research interests are silicon-based group IV material growth and silicon photonics.

Buwen Cheng received the BS and MS degrees in condensed physics from Beijing Normal University, China in 1989 and 1992, respectively, and the PhD degree from the Institute of Semiconductors, Chinese Academy of Sciences (ISCAS), China in 2006. He joined the ISCAS in 1992. Since 2007, he has been a professor. His current research interests include the growth of Si-based materials (such as SiGe, Ge, and GeSn) and device applications. He has authored or co-authored more than 150 journal articles and holds 15 patents.

Jun Zheng received the BEng degree from the Beijing Institute of Technology, China in 2006, and the PhD degree in physical electronics from the Graduated University of Chinese Academy of Sciences, China in 2011. He is now an associate researcher at the Institute of Semiconductors, Chinese Academy of Sciences, China. His main research interest is silicon photonics, especially silicon-based materials and detectors.

Zhi Liu received the BEng degree from Taiyuan University of Technology, China in 2009, and the PhD degree from the Institute of Semiconductors, Chinese Academy of Sciences, China in 2014. Since 2014, he has been working at the Institute of Semiconductors, Chinese Academy of Sciences, China. His research interests include silicon-based group IV material growth and silicon photonics. He has authored or co-authored more than 30 journal articles.

Yuhua Zuo received the BEng and MEng degrees from Tsinghua University, China in 1997 and 2000, respectively, and the PhD degree in microelectronics and optoelectronics from the Institute of Semiconductors, Chinese Academy of Sciences, China in 2003. She is a professor at both the University of Chinese Academy of Sciences and the Institute of Semiconductors, Chinese Academy of Sciences. She worked as a visiting scholar at the Department of Materials, University of California at Los Angeles, USA, for eight months in 2016. She has extensive research expertise and a wide range of research interests in novel Si-based optoelectronics materials and devices, such as photodiodes, APDs, and solar cells.